4380 *Chem. Mater.* **2009,** *21,* 4380–4386
DOI:10.1021/cm900628j

CHEMISTRY OF MATERIALS
Article

Organic Thin-Film Transistors Based on Blends of Poly(3-hexylthiophene) and Polystyrene with a Solubility-Induced Low Percolation Threshold

Longzhen Qiu,[†] Xiaohong Wang, Wi Hyoung Lee, Jung Ah Lim, Jong Soo Kim, Donghoon Kwak, and Kilwon Cho*

Department of Chemical Engineering, Pohang University of Science and Technology, Pohang, 790-784, Korea. [†]Current address: Key Laboratory of Special Display Technology, Ministry of Education, Academy of Opto-Electronic Technology, Hefei University of Technology, Hefei 230009, China.

Received March 5, 2009. Revised Manuscript Received August 23, 2009

We have demonstrated that organic thin-film transistors based on blends of poly(3-hexylthiophene) (P3HT) and polystyrene (PS) with high performance and low percolation threshold can be facilely fabricated by changing the solubility of solvent and the aging time of the precursor solution. The structural analysis reveals that these benefits arise from the improvements of both the crystallinity and connectivity of P3HT phase in the blend. In the case of crystallinity, we found that because of the solubility-aging-induced formation of ordered precursors, the molecular ordering of the poly(3-hexylthiophene) phase in the blend films increases, and thus the electronic properties of field-effect transistors (FETs) based on these films are significantly improved. For the connectivity, we found that either bilayered structure or highly connected P3HT nanofibrillar network could form in the blend by changing the solubility of the solvent. Both structures are extremely beneficial to keeping connectivity of active channels and thus keeping the charge-transport properties at low semiconductor content. By optimizing the conditions, the devices based on P3HT/PS blend films containing only 1 wt % P3HT can still show field-effect mobility as high as 1×10^{-2} cm^2V^{-1} s^{-1}, which is comparable with that obtained from the pristine P3HT film.

Introduction

In the past decade, the research of organic field-effect transistors (OFETs) has proceeded rapidly,[1] and now applications that require modest transistor performance, such as flexible active-matrix displays, are entering the advanced stages of industrial commercialization.[2] Such technologies will gain wide acceptance only if such electronic devices can be produced at a significantly lower cost than current capital-intensive manufacturing technologies.[3] Blending semiconducting polymers with insulating polymers is an attractive method for reducing the materials cost because the electronic properties of semiconducting polymers are then combined with the low-cost characteristics of insulating polymers.[4] However, the presence of the insulating component tends to degrade the device performance because the insulating polymer "dilutes" the current density of the film.[5−8] This effect can be reduced only if the connectivity of the semiconducting component in the blend is retained in the channel region. The induction of vertical phase separation in the blend film is an effective approach to achieving this goal. By using semiconducting/insulating polymer composites with vertically phase-separated structures as active layers, researchers have prepared OFET devices with reduced

*Corresponding author. Phone: +82-54-279-2270. Fax: +82-54-279-8298. E-mail: kwcho@postech.ac.kr.

(1) (a) Peng, X.; Horowitz, G.; Fichou, D.; Garnier, F. *Appl. Phys. Lett.* **1990**, *57*, 2013. (b) Bao, Z.; Dodabalapur, A.; Lovinger, A. J. *Appl. Phys. Lett.* **1996**, *69*, 4108. (c) Sirringhaus, H.; Tessler, N.; Friend, R. H. *Science* **1998**, *280*, 1741. (d) Crone, B.; Dodabalapur, A.; Lin, Y. Y.; Filas, R. W.; Bao, Z.; LaDuca, A.; Sarpeshkar, R.; Katz, H. E.; Li, W. *Nature* **2000**, *403*, 521. (e) Ong, B. S.; Wu, Y. L.; Liu, P.; Gardner, S. *J. Am. Chem. Soc.* **2004**, *126*, 3378. (f) McCulloch, I.; Heeney, M.; Bailey, C.; Genevicius, K.; Macdonald, I.; Shkunov, M.; Sparrowe, D.; Tierney, S.; Wagner, R.; Zhang, W. M.; Chabinyc, M. L.; Kline, R. J.; McGehee, M. D.; Toney, M. F. *Nat. Mater.* **2006**, *5*, 328. (g) Kobayashi, S.; Nishikawa, T.; Takenobu, T.; Mori, S.; Shimoda, T.; Mitani, T.; Shimotani, H.; Yoshimoto, N.; Ogawa, S.; Iwasa, Y. *Nat. Mater.* **2004**, *3*, 317. (h) Dickey, K. C.; Anthony, J. E.; Loo, Y. L *Adv. Mater.* **2006**, *18*, 1721. (i) DeLongchamp, D. M.; Vogel, B. M.; Jung, Y.; Gurau, M. C.; Richter, C. A.; Kirillov, O. A.; Obrzut, J.; Fischer, D. A.; Sambasivan, S.; Richter, L. J.; Lin, E. K. *Chem. Mater.* **2005**, *17*, 5610. (j) Ruiz, R.; Papadimitratos, A.; Mayer, A. C.; Malliaras, G. G. *Adv. Mater.* **2005**, *17*, 1795. (k) Meijer, E. J.; De Leeuw, D. M.; Setayesh, S.; Van Veenendaal, E.; Huisman, B. H.; Blom, P. W. M.; Hummelen, J. C.; Scherf, U.; Klapwijk, T. M. *Nat. Mater.* **2003**, *2*, 678.
(2) (a) Sanderson, K. *Nature* **2007**, *445*, 473. (b) Noh, Y. Y.; Zhao, N.; Caironi, M.; Sirringhaus, H. *Nat. Nanotechnol.* **2007**, *2*, 784.
(3) (a) Kim, C.; Wang, Z. M.; Choi, H. J.; Ha, Y. G.; Facchetti, A.; Marks, T. J. *J. Am. Chem. Soc.* **2008**, *130*, 6867. (b) Singh, T. B.; Sariciftci, N. S. *Annu. Rev. Mater. Res.* **2006**, *36*, 199–230. (c) Shtein, M.; Peumans, P.; Benziger, J. B.; Forrest, S. R. *Adv. Mater.* **2004**, *16*, 1615. (d) Baude, P. F.; Ender, D. A.; Haase, M. A.; Kelley, T. W.; Muyres, D. V.; Theiss, S. D. *Appl. Phys. Lett.* **2003**, *82*, 3964.
(4) Arias, A. C. *Polym. Rev.* **2006**, *46*, 103.
(5) Liu, J. S.; Sheina, E.; Kowalewski, T.; McCullough, R. D. *Angew. Chem., Int. Ed.* **2001**, *41*, 329.
(6) Babel, A.; Jenekhe, S. A. *Macromolecules* **2004**, *37*, 9835.
(7) Goffri, S.; Muller, C.; Stingelin-Stutzmann, N.; Breiby, D. W.; Radano, C. P.; Andreasen, J. W.; Thompson, R.; Janssen, R. A. J.; Nielsen, M. M.; Smith, P.; Sirringhaus, H. *Nat. Mater.* **2006**, *5*, 950.
(8) Sauve, G.; McCullough, R. D. *Adv. Mater.* **2007**, *19*, 1822.

Published on Web 09/17/2009

semiconductor costs, low-operating-voltage devices, and improved environmental stability and mechanical properties.[7,9−13] In a recent paper,[7] Goffri et al. reported that the concentration of the semiconductor in crystalline−crystalline bicomponent semiconductor−dielectric polymer systems can be reduced to a value as low as 3 wt % without any degradation in device performance.

Recently, we reported that inducing the semiconducting component to form embedded semiconducting nanofibers in the blends by using a marginal solvent represents an alternative means to obtain good field-effect electronic properties in devices based on blends with very low semiconductor contents.[14] The excellent connectivity and charge-transport properties of such nanofibers enables the reduction of the semiconductor content to as low as 3 wt % without considerable degradation of the field-effect electronic properties when compared to devices based on pristine P3HT prepared under the same conditions.

In this study, we systematically examined the influence of the solvent solubility on the morphology of thin films based on semiconducting and insulating polymer blends prepared from a solvent mixing method and on the electronic performance of OFETs based on these films. We found that the film morphology and electronic performance can be controlled by adjusting the ratio of the good and poor solvents for semiconducting component and the solution aging time. The relationship between the electronic properties and morphology has also been investigated.

Experimental Section

Materials and Sample Preparation. Regioregular P3HT (M_w = 40 kg mol^{-1}) was obtained from Rieke Metals Inc. Amorphous PS (M_w = 230 kg mol^{-1}), chloroform, dioxane, and cyclohexane were purchased from Aldrich Chemical Co. All materials were used as received without further purification. Field-effect transistors with a bottom-gate bottom-contact configuration were fabricated by using heavily doped n-type Si wafers as the gate electrodes and a 300 nm thick thermally grown silicon dioxide (SiO_2) layer (capacitance = 10.8 nF cm^{-2}) as the gate dielectric. The SiO_2 surface was cleaned in a piranha solution, washed with distilled water, and stored in a vacuum oven prior to electrode deposition. The gold source and drain electrodes (100 nm on a 2 nm adhesion layer of titanium) were deposited onto the silicon substrates by means of evaporation through shadow masks. The channel length and width were fixed at 100 and 800 μm respectively. P3HT/PS blend films with various P3HT contents were prepared by spin-coating from chloroform and dioxane mixed solutions (1.0 vol %). The cast films were dried at 60 °C in a vacuum oven to remove the residual solvent. To check the bottom surface of blend film with atomic force microscope (AFM), we floated the films onto the surface of a 5 wt % hydrogen fluoride solution, transferred them to a water bath, and then reversed them by slowly dipping a Si substrate into the solution from the center of the floated film.

Characterization. The electrical characteristics of the OFET devices were measured in the accumulation mode with Keithley 4200 and 236 source/measure units at room temperature and under ambient conditions. The capacitance was determined with an Agilent 4284 precision LCR meter. The film morphologies were characterized by using an AFM (Digital Instruments Multimode) operating in the tapping mode and a field-emission scanning electron microscope (FE-SEM, Hitachi S-4800). Grazing incidence X-ray diffraction (GIXRD) and X-ray photoelectron spectra (XPS) measurements were performed on the 8C1 and 4B1 beamlines, respectively, at the Pohang Accelerator Laboratory (PAL) in Korea. Solution-state UV−vis absorption spectra were recorded using an UV−vis spectrophotometer (Varian, CARY-5000). Ar^+ plasma sputtering was applied by exposing the samples to Ar^+ plasma for 5 min with a power of 15 W at room temperature.

Results and Discussion

Semiconductor/insulator mother solutions were prepared by blending poly(3-hexylthiophene) (P3HT) and amorphous polystyrene (PS) in a mixed solvent containing chloroform (CF), which is a common solvent for both P3HT and PS, and dioxane (DI), which is a good solvent for PS but a poor solvent for P3HT. As the ratio of DI in the solvent increases, the color of the solution gradually changes from light orange to dark brown. Figure 1a shows the variation of the UV−vis absorption spectrum of a 1.0 vol % P3HT/PS (5/95) solution as a function of the concentration of dioxane in the mixed solvent. The spectrum of pristine chloroform solution shows absorption characteristics that are typical of P3HT in a good solvent, with only one peak at λ = 450 nm. No obvious changes are observed in the absorption spectra for those solutions with DI less than 10 vol %. Upon further addition of DI, additional low-energy absorption bands at λ = 510, 550, and 605 nm emerge, and their intensities increase as the proportion of DI in the mixed solvent increases. These bands are identical to those observed for solid P3HT films and thus indicate the presence of ordered aggregates of P3HT molecules in the solutions.[15,16] After aging for 72 h, the intensities of the low-energy bands increase markedly for solutions with DI concentrations ranging from 10−30 vol % (see Figure 1b), which indicates an increasing of ordered aggregates with aging time. However, no obvious change can be observed in the absorption spectra of solutions containing too little (< 5 vol %) or too much (e.g., 50 vol %) DI.

Field-effect characteristics were measured in the bottom-contact, bottom-gate thin-film transistor (TFT) geometry using a 300 nm thick SiO_2 as the dielectric layer.

(9) Chua, L. L.; Ho, P. K. H.; Sirringhaus, H.; Friend, R. H. *Adv. Mater*. **2004**, *16*, 1609.
(10) Arias, A. C.; Endicott, F.; Street, R. A. *Adv. Mater*. **2006**, *18*, 2900.
(11) Muller, C.; Goffri, S.; Breiby, D. W.; Andreasen, J. W.; Chanzy, H. D.; Janssen, R. A. J.; Nielsen, M. M.; Radano, C. P.; Sirringhaus, H.; Smith, P.; Stingelin-Stutzmann, N. *Adv. Funct. Mater*. **2007**, *17*, 2674.
(12) Salleo, A.; Arias, A. C. *Adv. Mater*. **2007**, *19*, 3540.
(13) Qiu, L. Z.; Lim, J. A.; Wang, X. H.; Lee, W. H.; Hwang, M.; Cho, K. *Adv. Mater*. **2008**, *20*, 1141.
(14) Qiu, L. Z.; Lee, W. H.; Wang, X. H.; Kim, J. S.; Lim, J. A.; Kwak, D.; Lee, S.; Cho, K. *Adv. Mater*. **2009**, *21*, 1349.
(15) Ma, L.; Lee, W. H.; Park, Y. D.; Kim, J. S.; Lee, H. S.; Cho, K. *Appl. Phys. Lett*. **2008**, *92*, 063310.
(16) Berson, S.; De Bettignies, R.; Bailly, S.; Guillerez, S. *Adv. Funct. Mater*. **2007**, *17*, 1377.

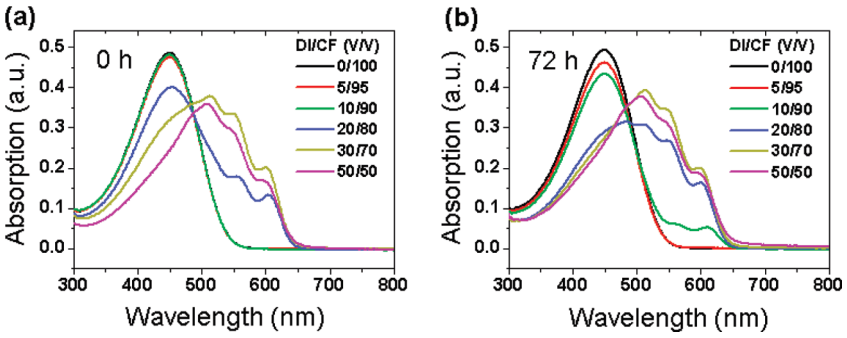

Figure 1. Absorption spectra of 1.0 vol % P3HT/PS (5/95) solutions of dioxane (DI) /chloroform (CF) mixtures with various solvent ratios and aging times: (a) 0 and (b) 72 h.

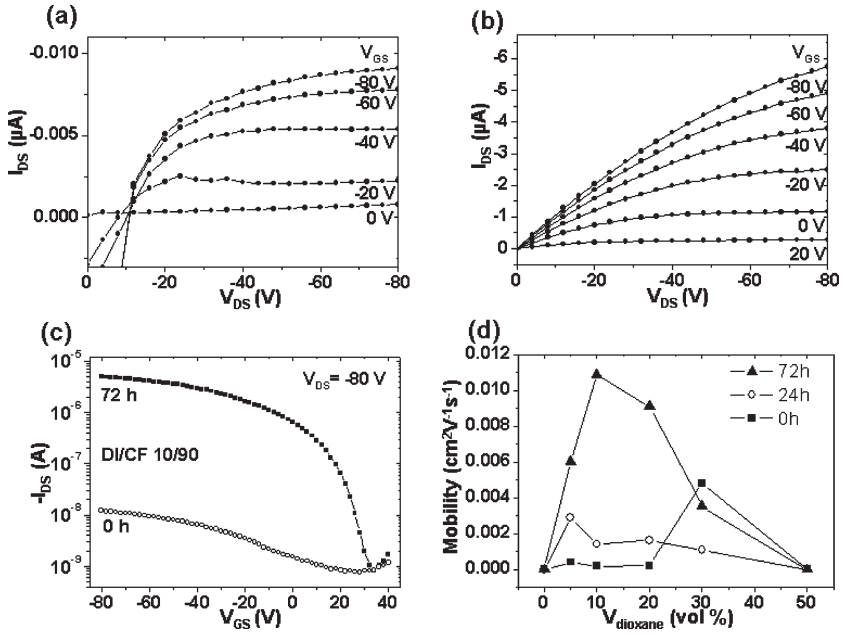

Figure 2. Field-effect transistor performance of P3HT/PS (5/95) blend films prepared from DI/CF mixtures with various aging times. I_{DS} is the drain−source current, V_{DS} is the drain−source voltage, and V_{GS} is the gate−source voltage. (a) Output characteristics of a device based on a blend prepared from a DI/CF (10/90) solution with 0 h of aging. (b) Output characteristics of a device based on a blend prepared from a DI/CF (10/90) solution with 72 h of aging. (c) Typical transfer characteristics of devices based on blend films prepared from DI/CF (10/90) solutions with 0 and 72 h of aging. (d) Average field-effect mobilities measured in the saturation region as a function of the DI ratio in the mixed solvent for various aging times.

The dielectric surface was bare without any organosilane treatment. The average mobility was calculated from more than 20 devices. Figure 2 shows the field-effect characteristics of the P3HT/PS (5/95) blend films prepared from solutions with various DI concentrations and aging times. As previously reported,[6,7] no field-effect characteristics can be observed in the P3HT/PS (5/95) blend films prepared from pristine chloroform solutions with or without aging because the P3HT content is below the percolation threshold (i.e., about 10 wt %). In stark contrast, all the films obtained from the DI/CF solutions show obvious field-effect characteristics. The performance of the devices based on these films is highly dependent on both the DI concentration and the aging time (Figure 2c and d). For those samples prepared from the solution with an aging time of 0 h, the mobility of the device increases with increases in the DI concentration up to 30 vol %. A maximum mobility of 4×10^{-3} cm^2 V^{-1} s^{-1} was observed for the blends prepared from the solution with DI. Aging the solutions result in obvious changes in the electronic performance of the samples prepared from the mixed solvents. Interestingly, the influence of aging on the electronic properties has a strong dependence on the DI concentration. For the films obtained from the solution with a DI concentration lower than 20 vol %, the field-effect performances of the devices improve rapidly as the aging time increases. As shown in Figure 2a−c, after aging the solution with 10 vol % DI for 72 h, the saturation drain current of the device increases by a factor of approximately 1×10^4 with respect to that of the sample without aging. However, for those samples obtained from solutions with a DI concentration higher than 30 vol %, the electronic properties do not change significantly, even degradation, with the increase of aging time.

Because the transport of charge carriers can only occur in the semiconductor component of a blend film, the electronic properties of the blends are totally dependent on that of the P3HT phase. To achieve high field-effect mobility in the blends, there are two critical factors. One is

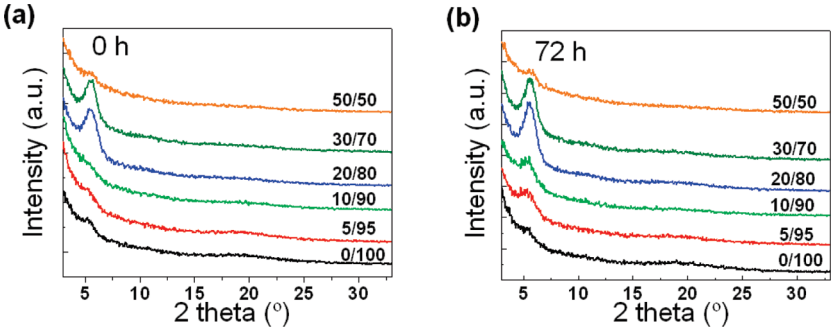

Figure 3. GIXRD patterns of P3HT/PS (5/95) films spin-cast from DI/CF mixed solutions with various solvent ratios and aging times: (a) 0 and (b) 72 h.

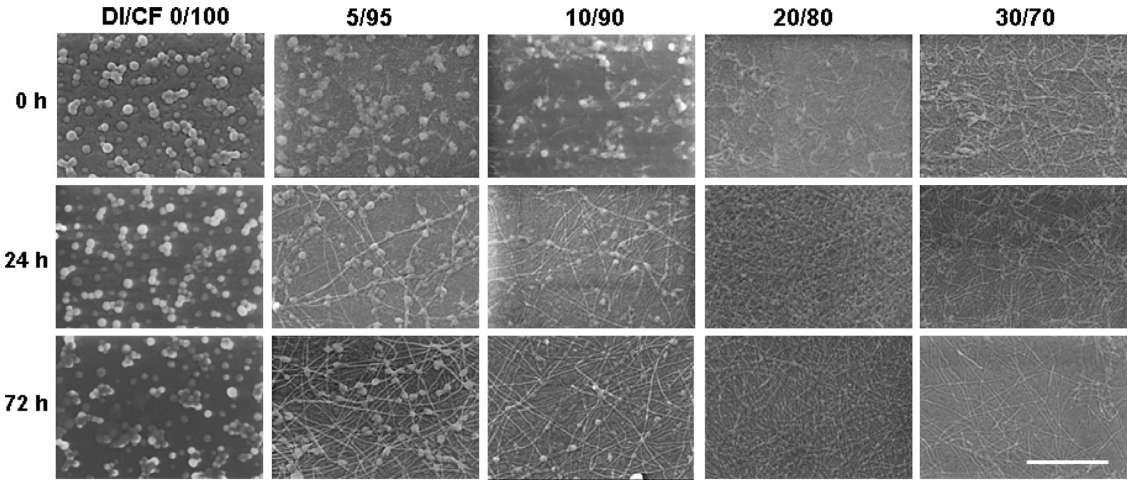

Figure 4. SEM images of P3HT/PS (5/95) films prepared from DI/CF mixed solutions with various solvent ratios and aging times after selectively removing PS with cyclohexane. The scale bar is 1 μm.

the crystalline structure of P3HT phase, which determine the charge-transport capability in the P3HT domain. The other is the morphology of P3HT phase, which determines the connectivity of active channel composed of P3HT domains. Therefore, GIXRD measurements were applied on the blend films, to investigate the influence of solubility and aging time on the crystalline structure and molecular orientation of the P3HT component in the blend films. As shown in Figure 3a, the GIXRD pattern of the sample prepared from a pristine CF solution contains a very weak and broad (100) diffraction peak due to P3HT. The addition of less than 10 vol % DI has little effect on the GIXRD pattern. However, as the amount of DI added to the solution increases above 20 vol %, the intensity of the (100) diffraction peak increases dramatically, which indicates that the crystallinities of the P3HT phase in these films is much higher than that of the film spin-cast from CF solution. The (100) peak indicates that the P3HT molecules adopt edge-on structures with their (100) axis normal to the substrate, which is extremely beneficial for charge transport in TFT devices.[17−19] As the DI concentration increases further to 50 vol %, the intensity of the (100) peak decreases significantly. After aging for 72 h, the intensity of the (100) diffraction peak increases in the samples prepared from solutions with DI concentrations ranging from 5−20 vol % (see Figure 3b), which indicates there is an increase in the crystallinity of the P3HT phase with aging time. However, there were no obvious changes in the patterns of those samples prepared from pristine CF solutions and those samples prepared from solutions containing DI concentration higher than 30 vol %.

Obviously, GIXRD results reveal that the increase of both the ratio of poor solvent and the aging time can increase the crystallinity of P3HT phase, which is consistent with the observations of improvement in field-effect mobility in Figure 2. Upon comparing the UV−vis spectra (Figure 1) and GIXRD (Figure 3) results, one can find that they show very similar profiles with the change of solubility and aging time. Therefore, we can conclude that the improved crystallinity of P3HT is derived from the ordered P3HT precursor constructed in blend solutions.

To investigate the morphology of P3HT phase, we selectively removed the PS phases of the samples by immersing them in cyclohexane for 10 min. Cyclohexane is a good solvent for PS, but does not dissolve P3HT. Scanning electron microscopy (SEM) (Figure 4) was used to elucidate the morphology of the remaining P3HT phase. Isolated spherical P3HT domains with a diameter

(17) Kline, R. J.; McGehee, M. D.; Toney, M. F. *Nat. Mater.* **2006**, *5*, 222.
(18) Kim, D. H.; Park, Y. D.; Jang, Y.; Yang, H.; Kim, Y. H.; Han, J. I.; Moon, D. G.; Park, S.; Chang, T.; Chang, C.; Joo, M.; Ryu, C. Y.; Cho, K. *Adv. Funct. Mater.* **2005**, *15*, 77.
(19) Yang, H.; Shin, T. J.; Yang, L.; Cho, K.; Ryu, C. Y.; Bao, Z. N. *Adv. Funct. Mater.* **2005**, *15*, 671.

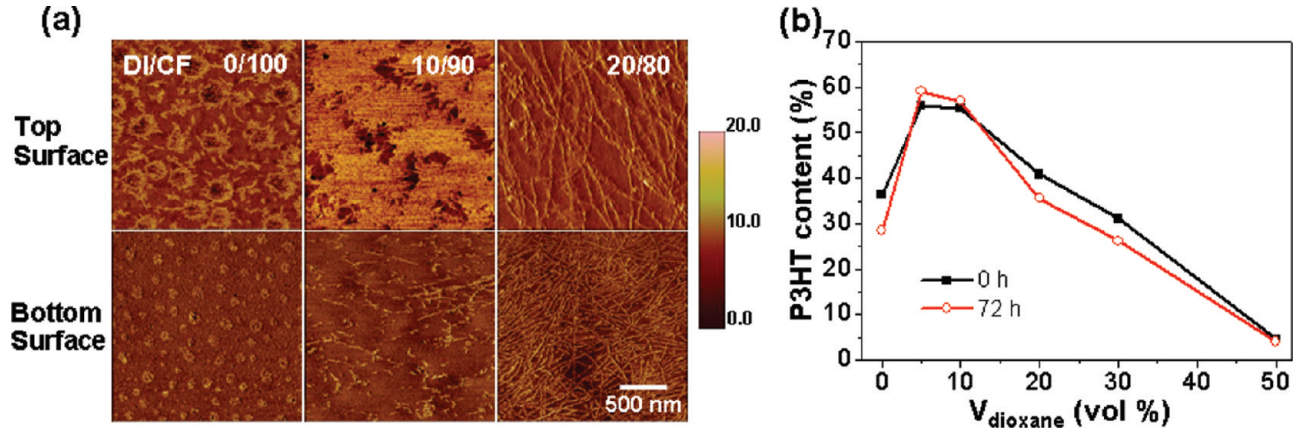

Figure 5. (a) AFM phase images of P3HT/PS (5/95) films spin-cast from DI/CF mixed solutions with various solvent ratios and 72 h of aging. (b) P3HT content of P3HT/PS (5/95) films (measured with XPS) as a function of the DI ratio in the mixed solvent.

of about 50−150 nm are observed for the samples obtained from pristine CF without aging. When 5 vol % DI is added into the solution, some short nanofibers begin to emerge. The number of nanofibers increases as the DI concentration in the mixed solvent increases. When the DI concentration in the mixed solvent is increased to 30 vol %, an interconnected nanofibrillar network of P3HT forms. It has been proved that the P3HT nanofibers exhibit an excellent 1D charge-transport along the nanofiber axis because the P3HT chains pack into a lamellar structure with two-dimensional conjugated sheets formed by interchain stacking perpendicular to the nanofiber axis.[19−21] Therefore, it is reasonable to ascribe the enhancement of the electronic properties to the P3HT nanofibers.

The P3HT morphology in the samples prepared form pristine chloroform is not significantly affected by solution aging. In contrast, a dramatic change occurs in the morphology of the samples prepared from the mixed solvent after the solutions have been aged. It was found that, with the increase in the aging time, the lengths of P3HT nanofibers increase rapidly, and form a highly interconnected network. These changes are extremely beneficial for charge transport because of the resulting increase in the connectivity and the decrease in the grain boundary of P3HT channels. As a result, the FET performances of the aged samples are significantly improved compared to the unaged samples (as shown in Figure 2). From the structural and morphological studies, we proved that P3HT ordered aggregates by decreasing the solubility of solvent in P3HT/PS blends lead to P3HT interconnected network embedded in PS matrix.

Interestingly, although the samples obtained from the solution with 10 vol % DI after aging for 72 h have higher field-effect mobility than the samples obtained from the solution containing 20 vol % DI prepared under the same conditions, the density of P3HT nanofibers in the former is much lower than that in the latter. It is possible that some P3HT structures were damaged when the samples were immersed into cyclohexane to selectively remove PS. To determine the original morphologies of the blend films, atomic force microscopy (AFM) measurements were performed on the top and bottom surfaces of the films (see Figure 5a). As is consistent with the SEM results, spherical and fibrillar P3HT domains, which appear lighter than PS in these images, are evident on both the top and the bottom surfaces of the P3HT/PS (5/95) films cast from pristine CF and the solution containing 20 vol % DI with an aging time of 72 h. However, in the case of the sample prepared from the solution containing 10 vol % DI, nearly full coverage P3HT layer is observed on the top surface, which is very different from the fibrillar structure observed in the SEM image. These results suggest that the morphology inside the film of P3HT prepared from the solution containing 10 vol % DI is quite different from that on the top surface.

XPS measurements were performed to evaluate the surface polymer composition of the blend thin films. Because only the P3HT molecules contain sulfur atoms, the sulfur compositions of the blend films can be compared to that of the homo-P3HT film to determine the P3HT ratio in the blend films. Figure 5b shows the relative P3HT ratio as a function of the DI concentration in the solvent for aging times of 0 and 72 h. It is clear that the surface composition is highly dependent on the DI concentration in the solvent. The P3HT contents on the surfaces of the blend films are 36% and 28% for the samples obtained from pristine CF solutions with aging time of 0 and 72 h, respectively, which are both much higher than the content of 5% in the solution. This surface enrichment of P3HT is driven by the difference between the surface energies of P3HT and PS (γ = 21.0[22] and 40.2 mJ m^{-2} [23] for P3HT and PS, respectively). It is well-known that the component with lower surface energy

(20) (a) Merlo, J. A.; Frisbie, C. D. *J. Polym. Sci., Part B: Polym. Phys.* **2003**, *41*, 2674. (b) Merlo, J. A.; Frisbie, C. D. *J. Phys. Chem. B* **2004**, *108*, 19169.
(21) Kim, D. H.; Jang, Y.; Park, Y. D.; Cho, K. *J. Phys. Chem. B* **2006**, *110*, 15763.
(22) Jaczewska, J.; Raptis, I.; Budkowski, A.; Goustouridis, D.; Raczkowska, J.; Sanopoulou, A.; Pamula, E.; Bernasik, A.; Rysz, J. *Syn. Met.* **2007**, *157*, 726.
(23) Tanaka, K.; Takahara, A.; Kajiyama, T. *Macromolecules* **1996**, *29*, 3232.

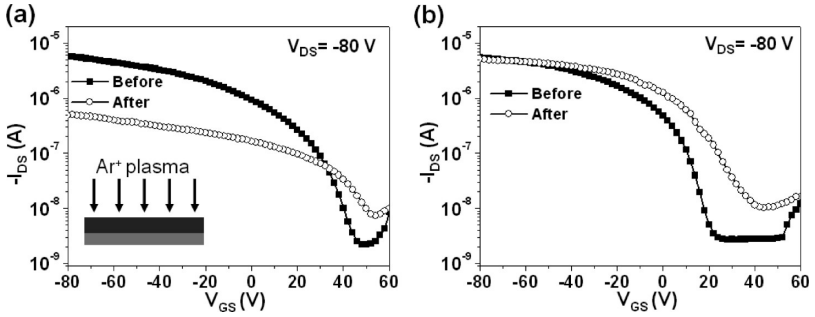

Figure 6. Typical transfer characteristics of FET devices based on P3HT/PS (5/95) films prepared from mixed solvents with DI/CF ratios of (a) 10/90 and (b) 20/80 before and after selectively removing the surface layer by exposure to Ar^+ plasma.

tends to segregate at the air−film interface in order to minimize the air−polymer surface tension.[24] Upon addition of 5−10 vol % DI into the blend solution, the P3HT content increases to ~60%. Further increases in the DI concentration result in a monotonic decrease of P3HT content on the surface. These results are consistent with the AFM observations. Although aging the solutions has drastic effects on the electronic properties and morphology of the prepared films, it has little influence on the surface composition.

The effect of solubility of solvent on the phase separation of the polymer blend during spin-coating process has been widely studied.[25] It has been found that the component with lower solubility is more quickly depleted from the solvent and solidified first on the substrate. The component with higher solubility tends to stay longer in the liquid phase and is enriched at the surface. However, in our case, surface enrichment of P3HT was observed when a poor solvent for P3HT, DI, was added at low concentrations (5−10%). To verify these results, the properties of solutions of the blends need to be taken into account because the formation of P3HT ordered aggregates in the solution can influence the phase-separation characteristics of the P3HT/PS blends. In the case of the film prepared from the pristine CF solution, lateral phase-separation occurs, as indicated by the SEM and AFM images. When CF evaporates during the spin-coating process, the nucleation of P3HT molecules occurs, and P3HT phase grow along the lateral direction. Because the concentration of P3HT in the solution is only 5%, the growth of P3HT phase is restricted by the supply of P3HT molecules, and thus results in isolated spherical P3HT domains. However, when DI is added at 5−10%, some P3HT ordered aggregates are formed in the solution as a result of the lower solubility of P3HT in DI, however, most of P3HT molecules are in the dissolved state (see Figure 1b). When the blend solution is deposited onto the substrate, P3HT molecules rapidly segregated at the air−film interface because it has a lower surface energy than PS. Because the ordered aggregates in the solution act as nucleation sites, P3HT solid form easily, and the growth rate of P3HT solid at the air−film interface is higher than for the film prepared from the pristine CF solution. Thus, at this solvent ratio, interconnected P3HT phase form at the surface and the surface of the final film is richer in P3HT than the bottom of the film. The increase of DI ratio to 20% further decreases the solubility of P3HT, and thus induce most of P3HT molecules exist as ordered aggregates in the solution (as indicated by the UV−vis spectra in Figure 1). The aggregated P3HT component tends to precipitate at the bottom during spin-casting because of the gravitational force. Therefore, the density of P3HT nanofibers at the bottom surface is much higher than that at the top surface (see the AFM images in Figure 5a). As the DI ratio increases to 30−50%, large P3HT aggregates emerge in the solution. For this reason, the motion of P3HT molecules to the top surface become very rare, resulting in a decrease in the P3HT content at the air−film interface, as confirmed by the XPS results (Figure 5b). Further experiments using time-resolved in situ characterization techniques are necessary to resolve the dynamic characteristic of the phase separation.

To investigate the effects of the structure of the blend films on their field-effect charge transport, surface layers of the blend films were selectively removed by exposing them to Ar^+ plasma. Figures 6a and b show the FET characteristics before and after treatment with Ar^+ plasma of the films prepared from solutions containing 10 vol % and 20 vol % DI. It can be seen that the saturation drain current in the sample prepared from the solution containing 10 vol % DI is degraded by a factor of approximately 10 after plasma treatment. This means that the active channel is close to the top surface of the blend film. In sharp contrast, the change in the field-effect performance of the blend prepared from the solution containing 20 vol % DI before and after plasma treatment was much smaller than that of the blend obtained from the solution containing 10 vol % DI, indicating the active channel is at the bottom layer of the blend film. Upon comparing the changes in field-effect performance before and after plasma treatment with the AFM and XPS results (see Figure 5), it is clear that the charge carriers

(24) (a) Heriot, S. Y.; Jones, R. A. L. *Nat. Mater.* **2005**, *4*, 782. (b) Boltau, M.; Walheim, S.; Mlynek, J.; Krausch, G.; Steiner, U. *Nature* **1998**, *391*, 877.

(25) (a) Walheim, S.; Boltau, M.; Mlynek, J.; Krausch, G.; Steiner, U. *Macromolecules* **1997**, *30*, 4995. (b) Ton-That, C.; Shard, A. G.; Bradley, R. H. *Polymer* **2002**, *43*, 4973. (c) Ton-That, C.; Shard, A. G.; Teare, D. O. H.; Bradley, R. H. *Polymer* **2001**, *42*, 1121. (d) Cui, L.; Ding, Y.; Li, X.; Wang, Z.; Han, Y. C. *Thin Solid Films* **2006**, *515*, 2038. (e) Dekeyser, C. M.; Biltresse, S.; Marchand-Brynaert, J.; Rouxhet, P. G.; Dupont-Gillain, C. C. *Polymer* **2004**, *45*, 2211. (f) Tanaka, K.; Takahara, A.; Kajiyama, T. *Macromolecules* **1995**, *28*, 934.

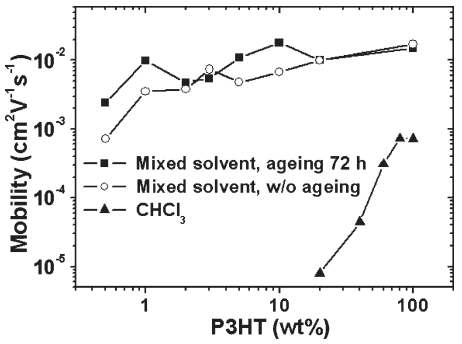

Figure 7. The average field-effect mobilities of FET devices based on P3HT/PS blend films as a function of P3HT content.

transport in the P3HT-rich top layer for the films obtained from solution containing 10 vol % DI, and in the embedded P3HT nanofibers for the films obtained from solution containing 20 vol % DI.

Figure 7 summarizes the average field-effect mobilities of the blend-based devices with various P3HT contents prepared with the solvent mixing method. As is consistent with previously reported results, the mobility of blend films spin-cast from CF solutions decreases monotonically as the P3HT content is decreased. Finally, a percolation threshold is observed at a concentration of approximately 20 wt %. Surprisingly, for the blends prepared from mixed solvents, the FET device performance is comparable to that of homo-P3HT films prepared under the same conditions even for semiconducting-polymer contents as low as approximately 1 wt %. These results are superior to previous results for semiconducting/crystalline-insulating polymer blends.[7]

Conclusions

We have systematically investigated the influence of the solubility of solvent and the aging of the solution on the morphology of thin films prepared from the blends of semiconducting P3HT and insulating PS using good/poor solvent (i.e., chloroform/dioxane) mixture and on the electric performance of OFETs based on these films. We found that P3HT ordered precursors form spontaneously in the solution with the decrease in solubility induced by the gradual addition of a poor solvent, and by increasing the aging time of the solution. As a result of this solubility-aging-induced formation of ordered precursors, the molecular ordering of the P3HT phase in the blend films increases, which is extremely beneficial for charge transport. Further measurements with SEM, AFM, and XPS show that the morphologies of the blend film are highly dependent on the solubility of solvent. In the case of P3HT/PS (5/95) blend, a morphology of isolated spherical P3HT domains in PS matrix formed in the films prepared from a chloroform solution; whereas a consecutive P3HT-riched top-layer and an embedded P3HT nanofibrillar network formed in the film prepared from the solutions with dioxane/chloroform ratio of 10/90 and 20/80, respectively. Both layered and nanofibrillar structures well-maintain the connectivity of the semiconducting component in the blend, and thus the FETs based on these blend films showed undeteriorated device performance when compared with devices comprising pristine P3HT. In remarkable contrast, the P3HT/PS (5/95) blend films obtained from a chloroform solution showed no FET characteristics. By optimizing the conditions, the devices based on polymer blends containing only 1 wt % semiconductor were fabricated with field-effect mobility as high as 1×10^{-2} cm^2 V^{-1} s^{-1}, which is comparable with that obtained for pristine semiconductors.

Acknowledgment. This work was supported by a grant (F0004021-2009-32) from the Information Display R&D Center under the 21st Century Frontier R&D Program, Creative Research Initiative-Acceleration Research (R17-2008-029-01001-0). The authors thank the Pohang Accelerator Laboratory for providing the synchrotron radiation sources at 4B1, 8C1, 8A2, and 10C1 beamlines used in this study.